

Flutter analysis with an Euler-based solver in OpenFOAM

Andrea Mannarino, presenter Sergio Ricci



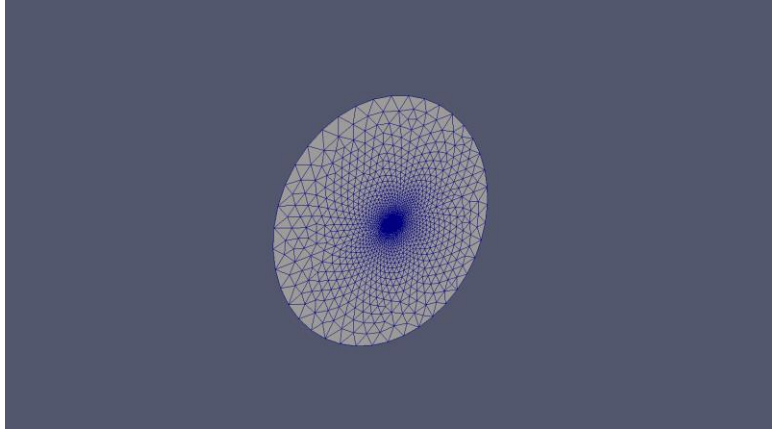
POLITECNICO
MILANO 1863

Politecnico di Milano
Department of Aerospace Science and Technology
Milano - Italy

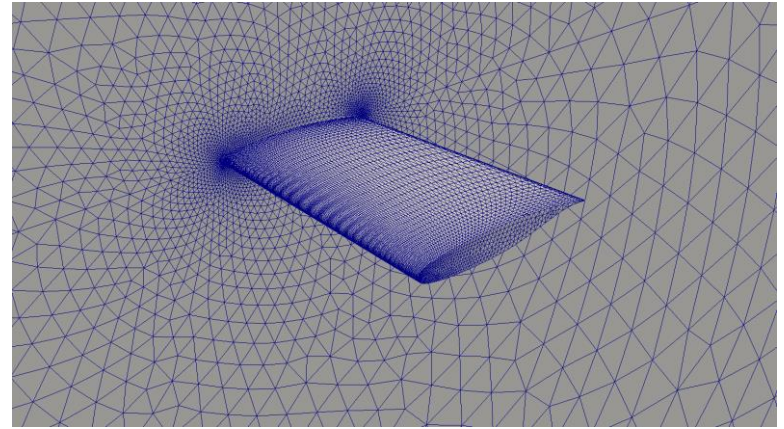
Table of contents

- ❑ Mesh generation
- ❑ Aerodynamic solver
- ❑ Flutter point estimation
- ❑ Results analysis
- ❑ Concluding remarks

Mesh generation



Semi-spheric domain

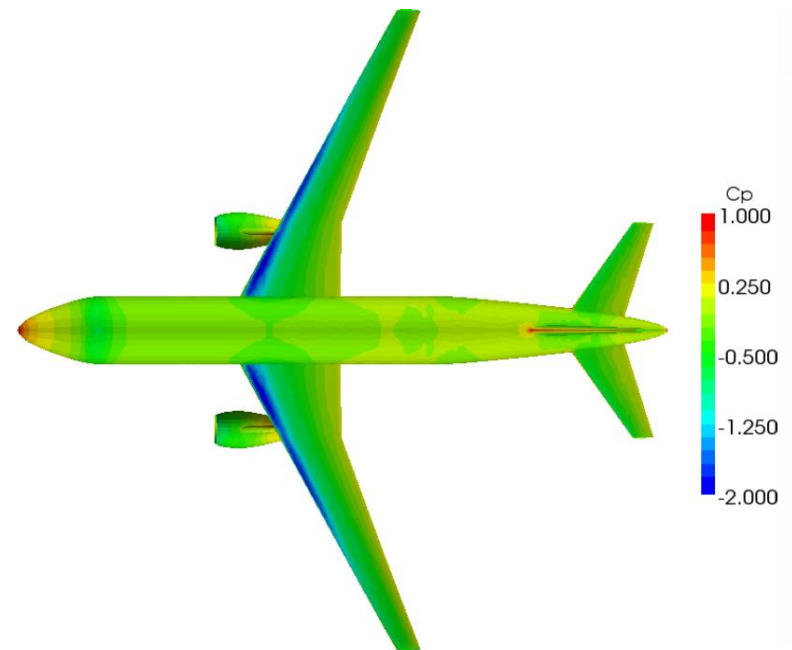
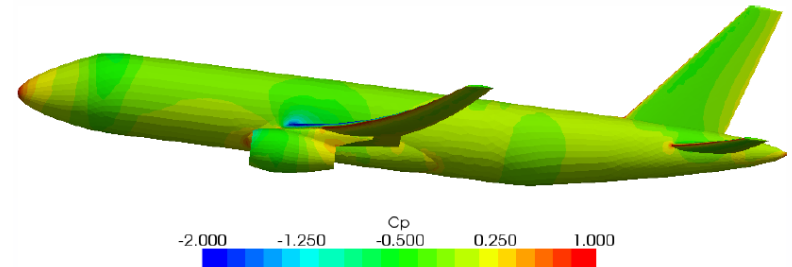


Wing close-up

- ❑ Problems in converting the provided meshes to OpenFOAM
- ❑ Mesh created with Pointwise through the IGES file available on the AEPW2 project web site
- ❑ Spatial discretization of the domain:
 - Coarse mesh with 320k cells
 - Medium mesh with 690k cells

Aerodynamic solver: AeroFoam

- In-house solver developed at the DAST supported by OpenFOAM libraries
- RANS, cell-centered, density based solver for aero-servo-elastic applications
- First density-based RANS solver implemented in OpenFOAM to overcome the limits of the available pressure based solvers in transonic application



Aerodynamic solver: AeroFoam

- ❑ Euler-option is selected for the following simulations: viscosity and thermal conductivity effects are not modeled
- ❑ Convective fluxes are discretized by the Roe's approximated Riemann solver, blended by the centered approximation of Lax-Wendroff
- ❑ Entropy fix of Harten and Hyman and van Leer flux limiter
- ❑ Time discretization performed by an explicit multi-step Runge-Kutta scheme of the 5th order
- ❑ Combined dual-time stepping and a full-approximation storage multi-grid technique to speed up the convergence between time steps

Simulation settings

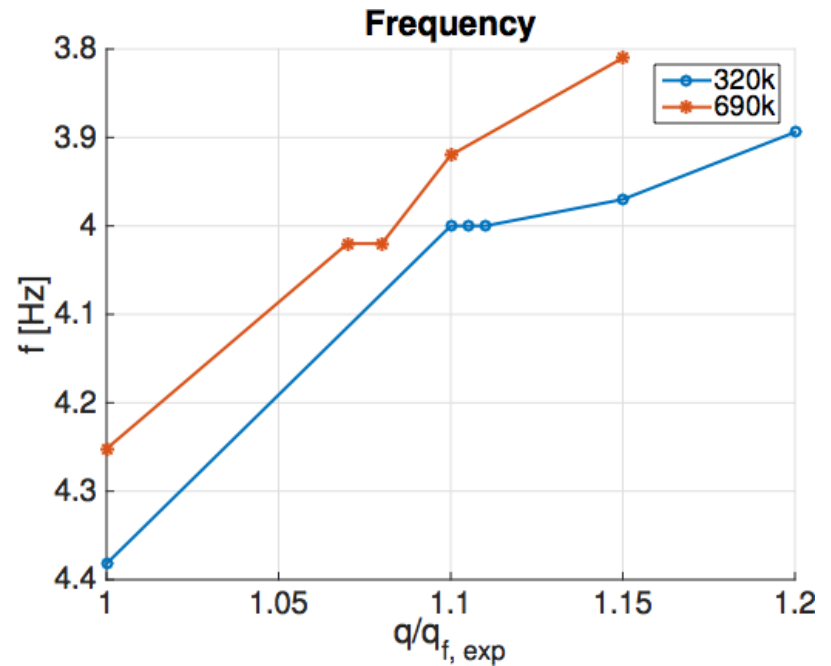
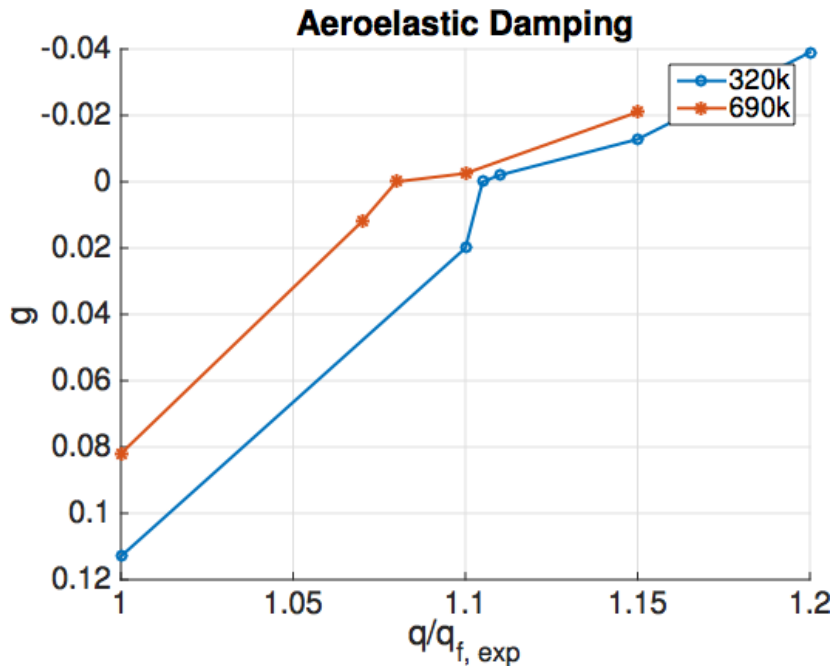
Aeroelastic interface

- ❑ Mode shapes downloaded from the AEPW2 project web site
- ❑ Because the wing is rigid, the mesh is translated and rotated rigidly during the simulation
- ❑ The coupling between structural and aerodynamic models is performed at each time step through a linear method

Aerodynamic solver parameters

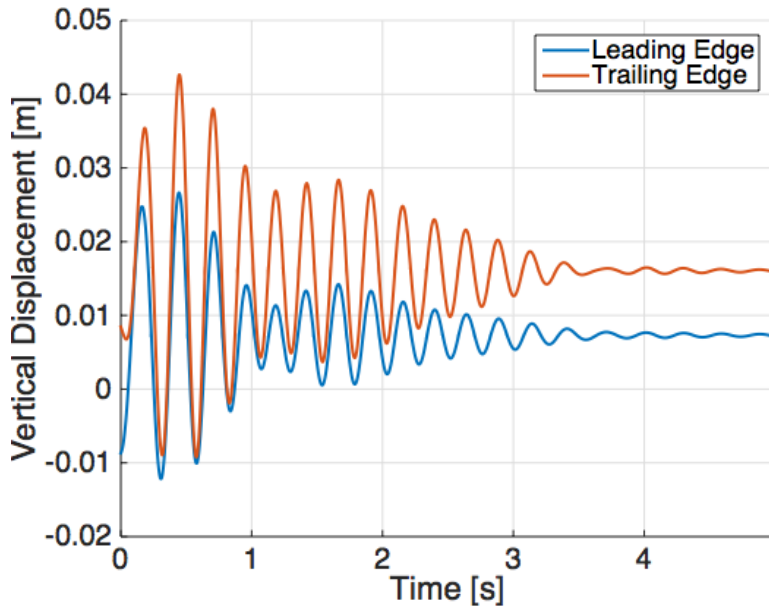
- ❑ Time step convergence analysis: $1e-3$, $5e-4$, $2.5e-4$ s
- ❑ CFL set to 2.0
- ❑ 1000 iterations in pseudo-time are allowed between each time step
- ❑ Two multi-grid levels are used (V-cycle)

Flutter point estimation

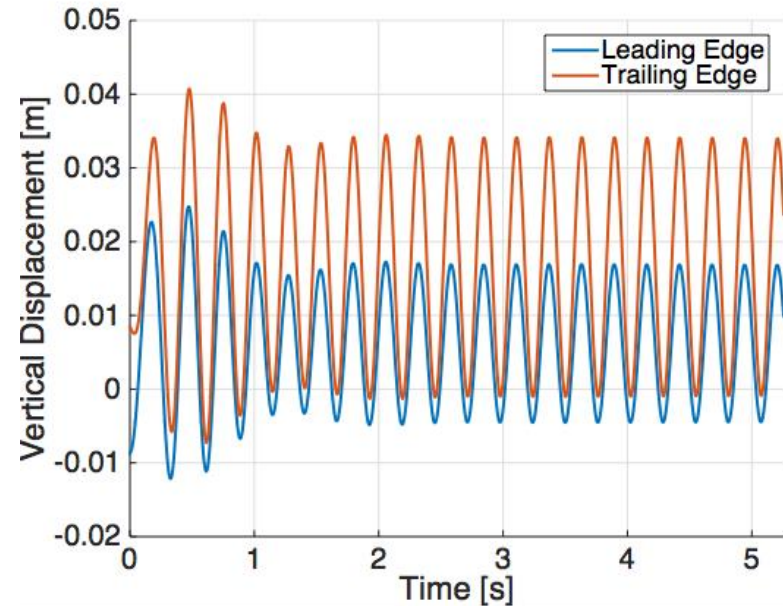


- ❑ Flutter point always overestimated vs experimental value
- ❑ Error on flutter frequency smaller than damping
- ❑ Flutter point for 320k mesh -> 1.105 experimental value
- ❑ Flutter point for 690k mesh -> 1.080 experimental value
- ❑ Flutter frequency always around 4 Hz

Experimental vs numerical flutter



Experimental

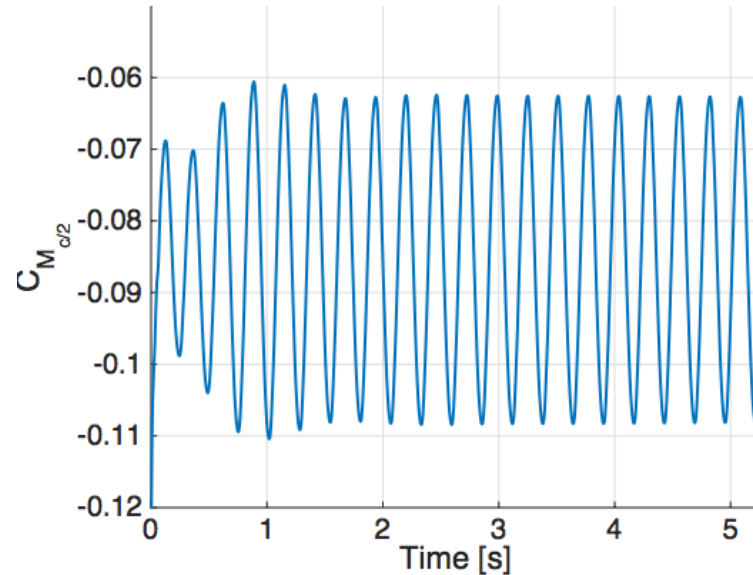
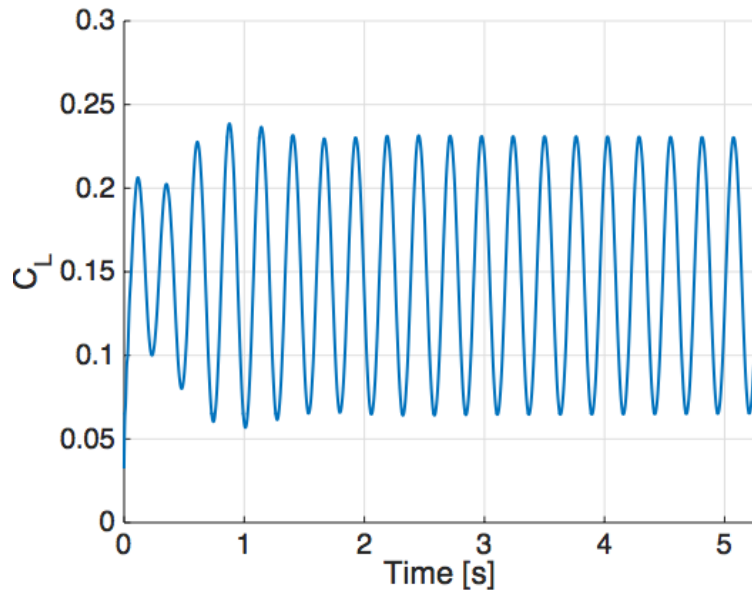


Numerical

Temporal convergence at flutter speed

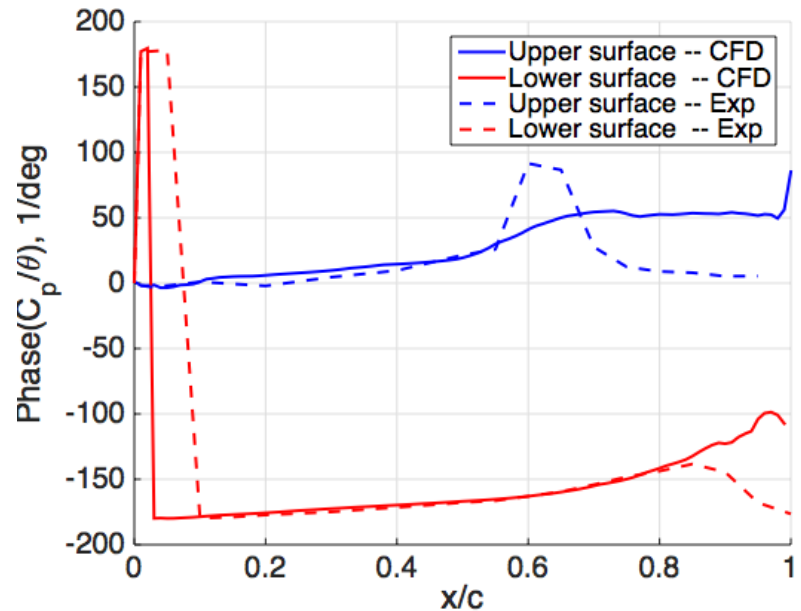
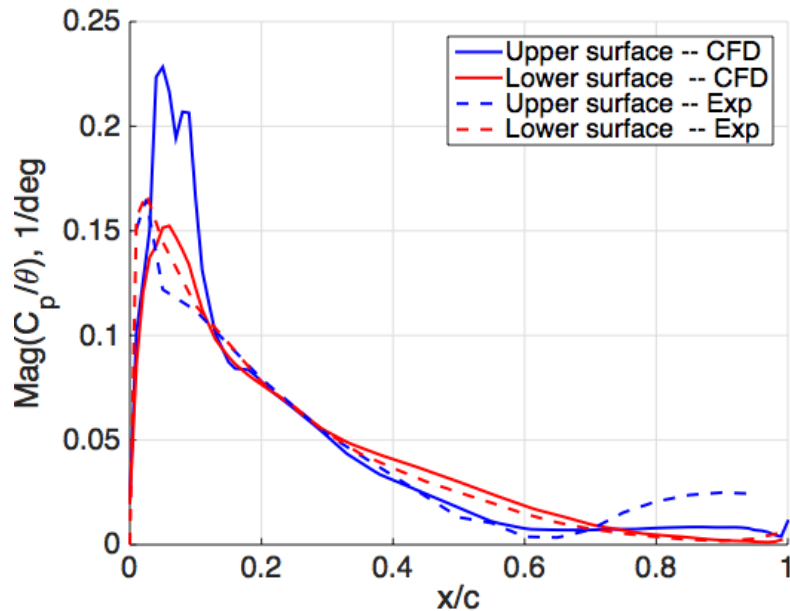
- ❑ Damping variation from $dt = 1e-3$ to $5e-4$
- ❑ No variation of damping from $dt = 5e-4$ to $2.5e-4$

Analysis of the flutter solution



- ❑ The oscillations are not symmetric with respect to the origin
- ❑ The average angle of rotation is negative
- ❑ The average wing plunge is positive

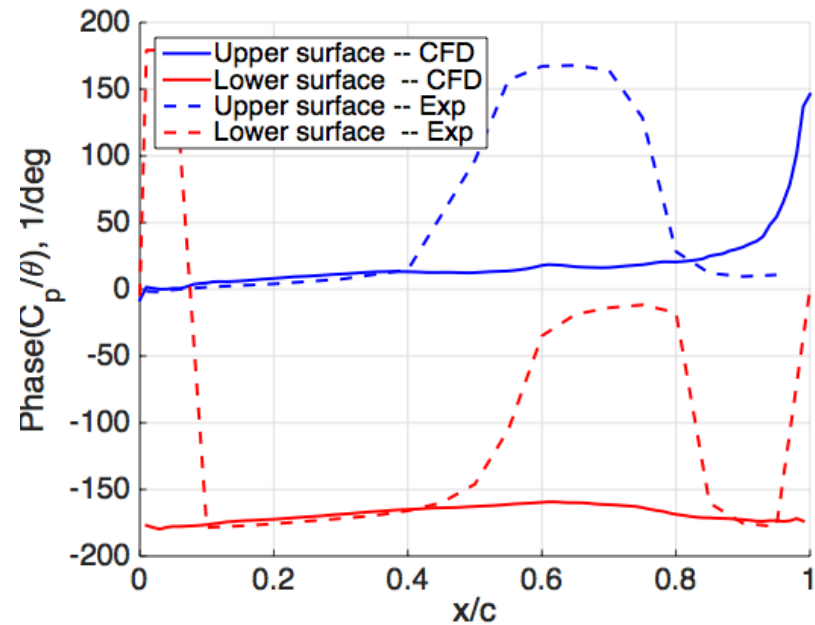
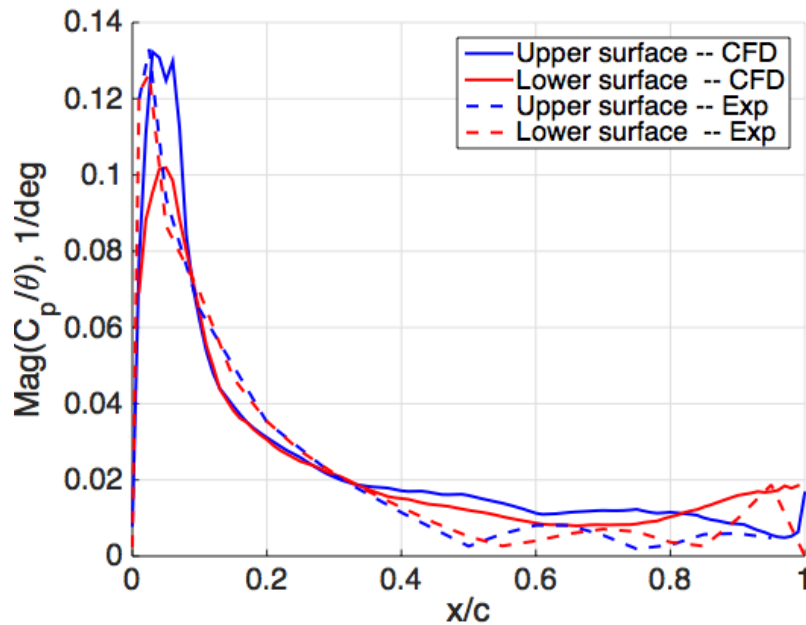
Load distribution at computational flutter



FRF @ 60% span

- ❑ The computational model presents a higher peak on the upper surface
- ❑ Phase predicted with good accuracy, missing effect at 60% chord, probably due to boundary layer transition

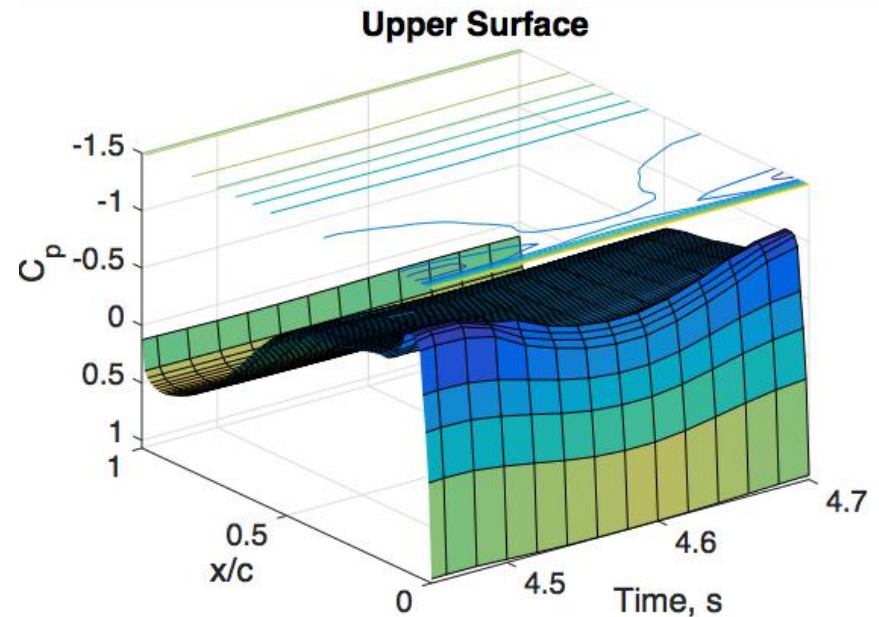
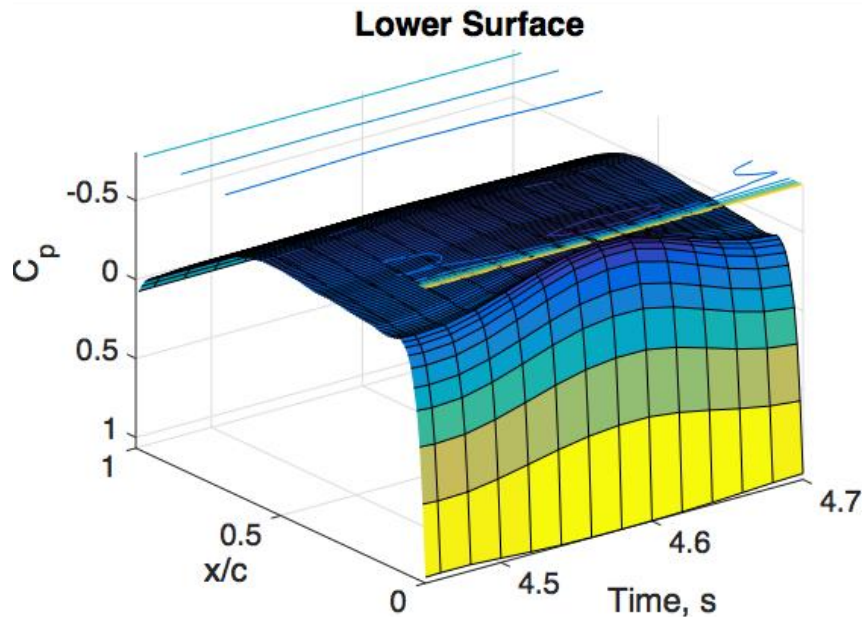
Load distribution at computational flutter



FRF @ 95% span

- ❑ The computational model presents a smaller peak on the lower surface
- ❑ Phase not well predicted, still missing effect at 60% chord, probably due to boundary layer transition

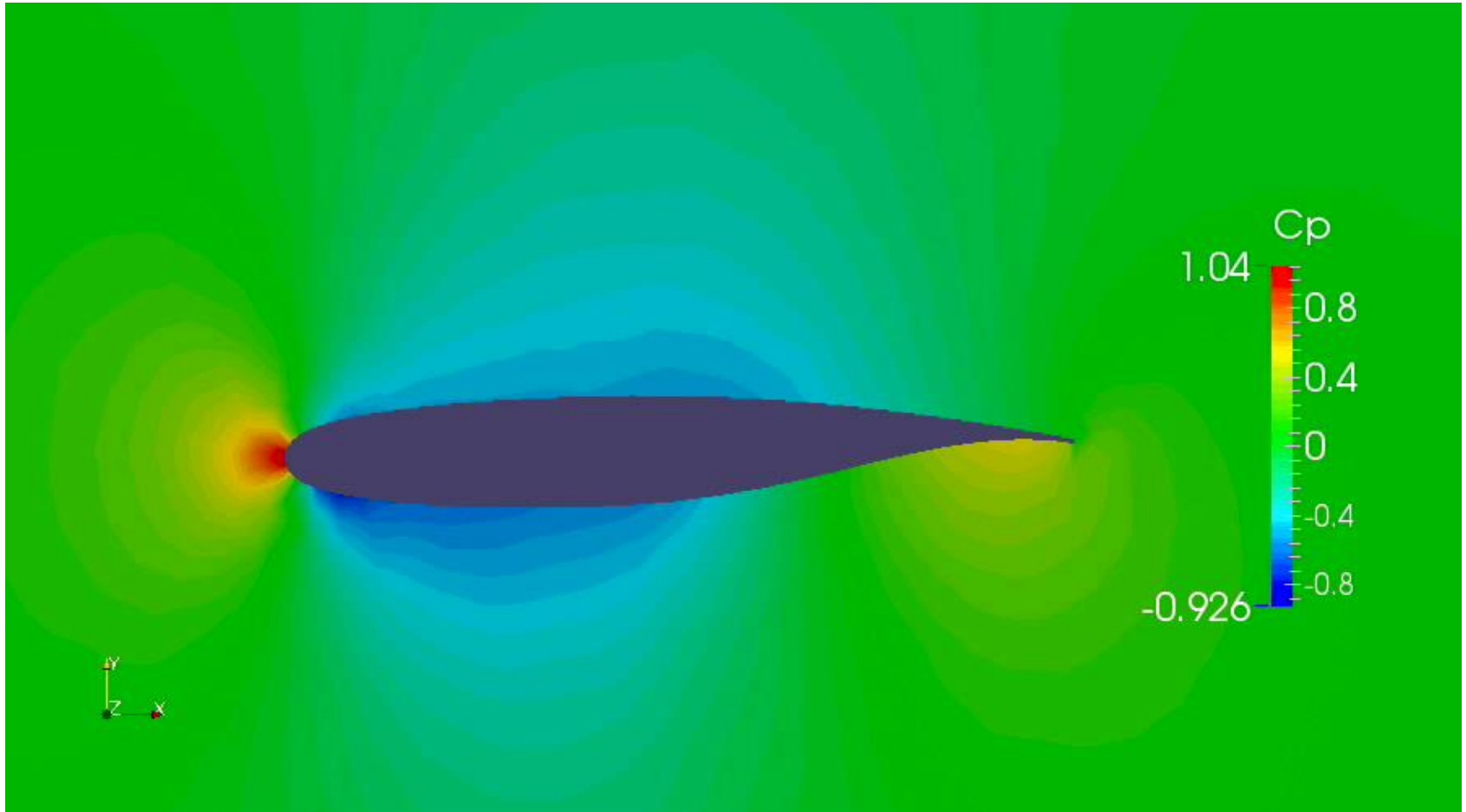
Load distribution vs time



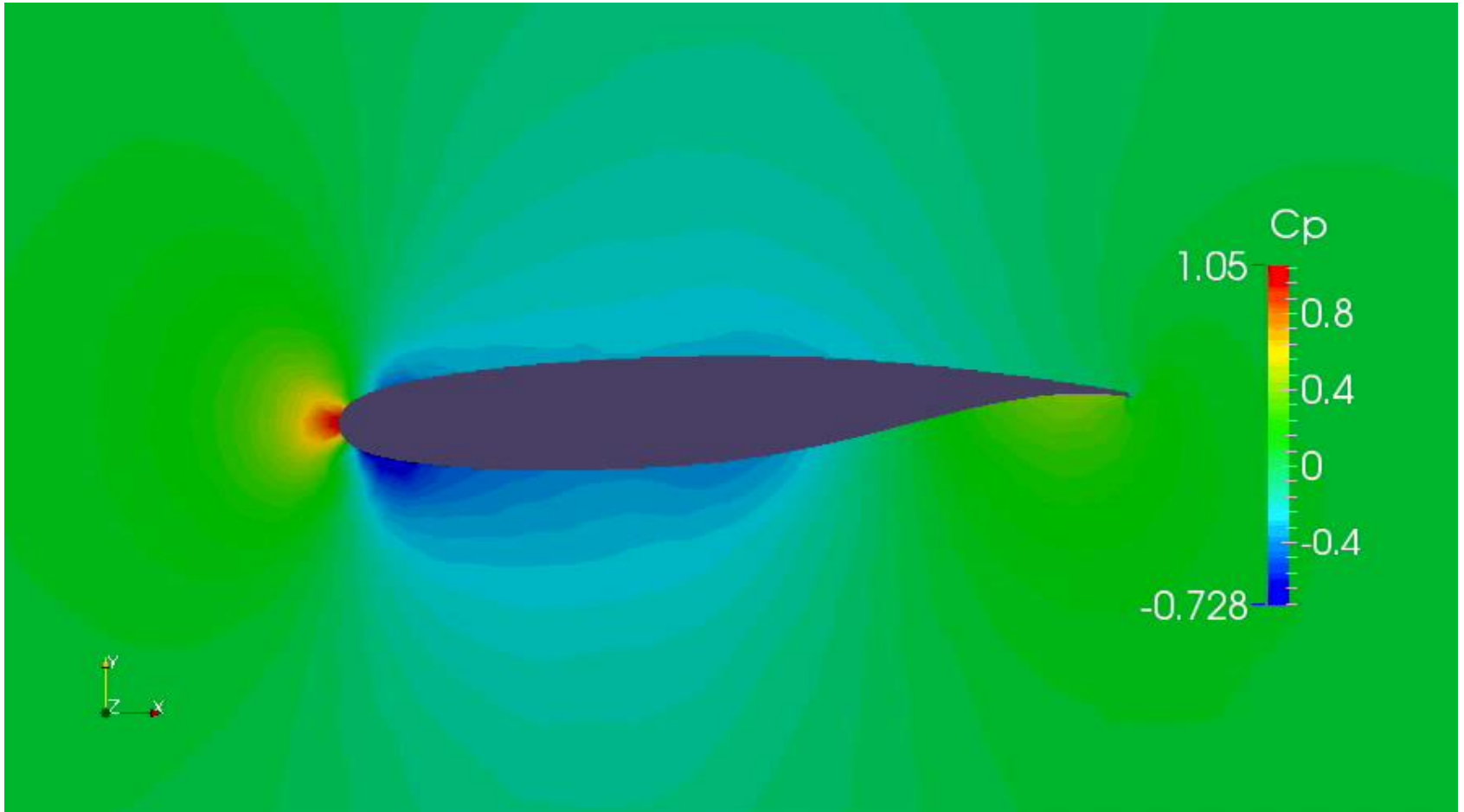
C_p @ 60% span

- ❑ A weak shock moves back and forth the chord on both surfaces
- ❑ A narrow peak is present on the leading edge of the upper surface

Pressure field @ 60% span



Pressure field @ 95% span



Concluding remarks

- ❑ Euler-based flutter simulations have been presented
- ❑ Good accuracy in flutter estimation (error smaller than 10%) has been found
- ❑ The flutter point is always overpredicted with respect to the experimental value
- ❑ Not so accurate in load distribution predictions, probably due to non-modeled effects
- ❑ Additional analyses with refined meshes should be carried out to confirm the convergence toward the flutter predicted by the experiments

Thank you!!!
Any question?

Cases under investigation

case 1) Mach = 0.7

AoA = 3°

Dynamic data type = Forced oscillation, $f = 10\text{Hz}$, $|\theta| = 1^\circ$

notes: attached flow, OTT exp data, R-134°

case 2) Mach = 0.74

AoA = 0°

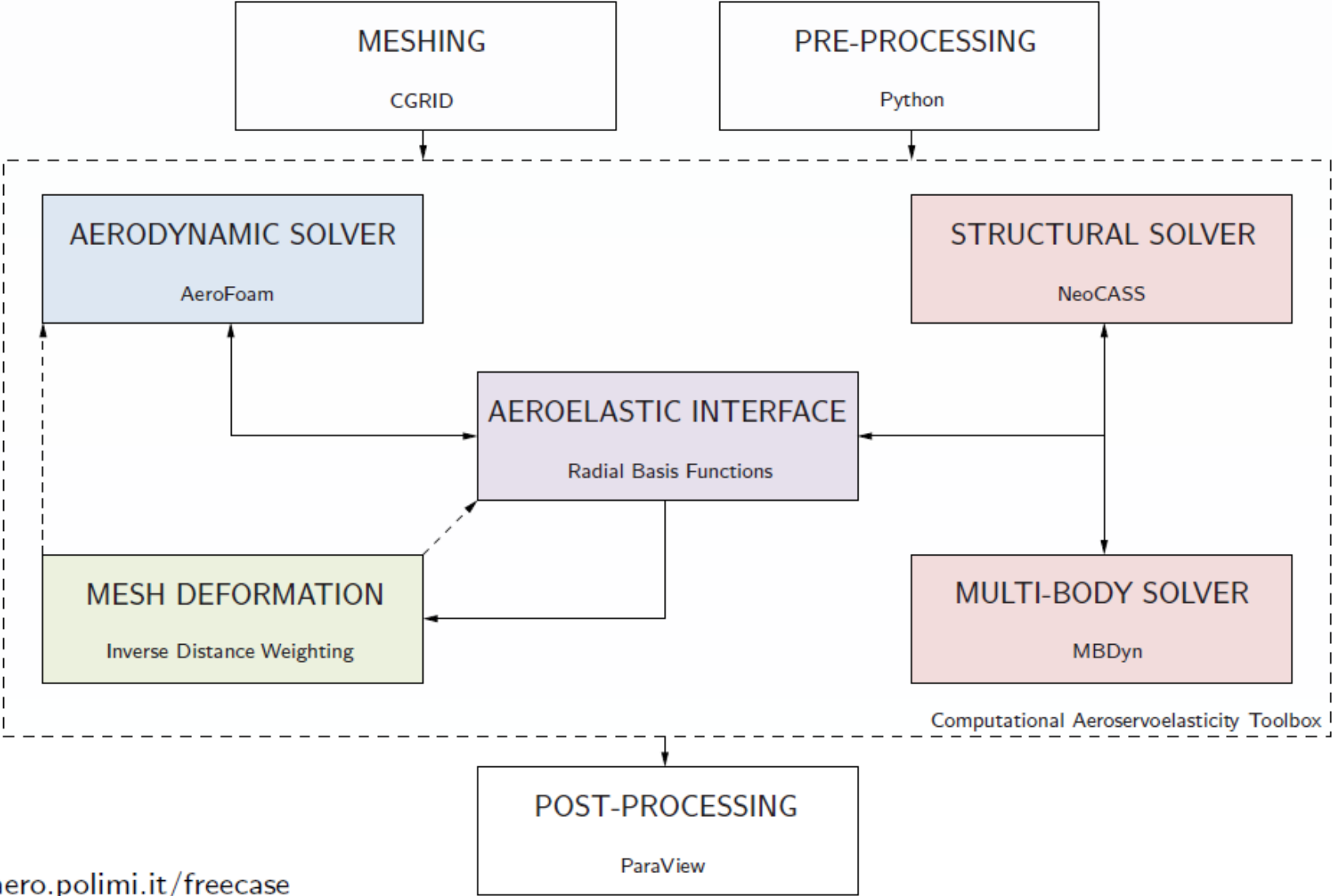
Dynamic data type = Flutter

notes = flow state unknown, PAPA exp. data, R-12

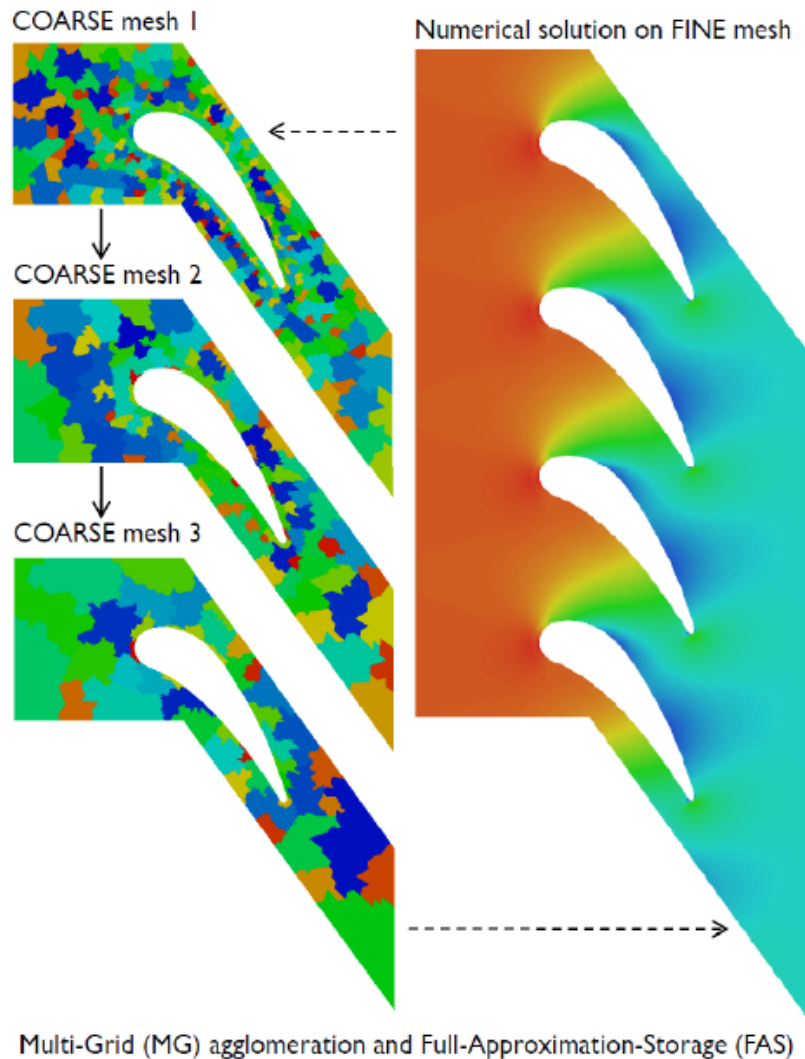
Solver:

- Explicit - dual time stepping
- density based
- euler / rans (spalart allmaras / SST)
- grid deformation / traspiration
- GPU

FreeCASE toolbox



AeroFoam



Motivation and objective:

- First density-based ALE RANS solver in OpenFOAM
- To overcome the limits of built-in pressure-based solvers in the transonic regime (e.g. sonicFoam)
- Benchmarking vs. EDGE and FLUENT

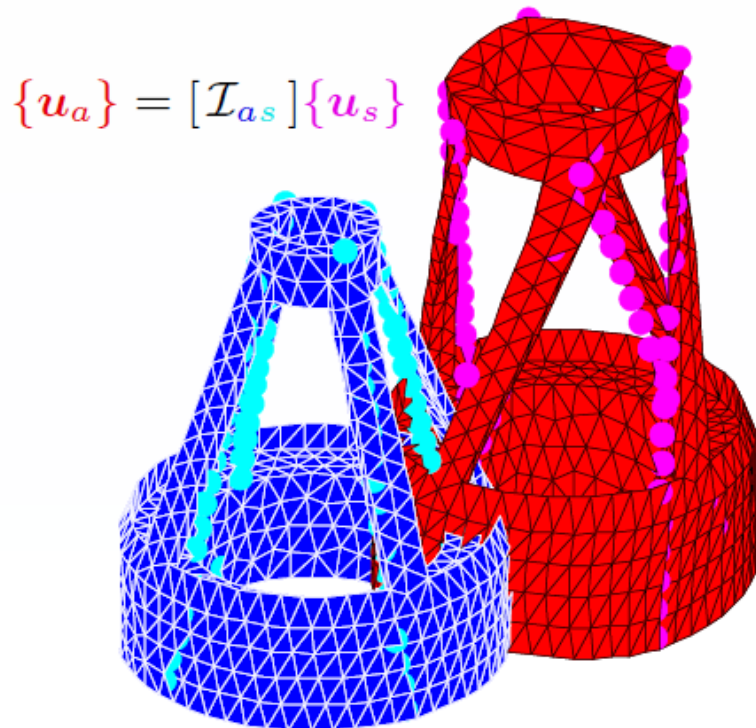
Features:

- Coupled formulation in conservative variables
- Space discretization (1st, 2nd order accuracy)
 - Roe's Approximate Riemann Solver (ARS)
 - Lax-Wendroff (LW) scheme with flux limiters
 - Directional Residual Smoothing (RS)
- Time discretization (1st, 2nd order accuracy)
 - Explicit multi-step Runge-Kutta (RK) scheme
 - Local Time-Stepping (LTS)
 - Double Time-Stepping (DTS)
 - Multi-Grid (MG) acceleration (FMG and FAS options)
- Automatic handling of parallel communication, cyclic boundaries, Generic Grid Interface (GGI)

FSI

Target: closed loop connection between structural and aerodynamic sub-systems

- projection (in PVW sense) of aerodynamic forces onto structural displacements
- translation of structural displacements into aerodynamic boundary conditions



Moving Least Squares (MLS):

- connect topologically different domains
- exact treatment of rigid motions
- accuracy, smoothness & efficiency trade-off

$$\text{Minimize } \int_{\Gamma} \phi(\text{Tr}(\mathbf{u}_a)|_{\Gamma} - \text{Tr}(\mathbf{u}_s)|_{\Gamma})^2 dS$$

- weighting via Radial Basis Functions (RBF)

A hierarchy of mesh deformation tools

R Least-squares identification of translation vector \mathbf{s} and linear map tensor \mathbf{T}

$$\Delta \mathbf{x}_j = \mathbf{s} + \mathbf{T} \mathbf{x}_j + \boldsymbol{\varepsilon}_j = \mathbf{s} + (\mathbf{R} - \mathbf{I}) \mathbf{x}_j + \mathbf{D} \mathbf{x}_j + \boldsymbol{\varepsilon}_j \quad \forall j \in [1, N_b]$$

easier to implement, rotation tensor follows: $(\mathbf{R} - \mathbf{I}) = s_\phi \mathbf{K}_\times + (1 - c_\phi) \mathbf{K}_\times \mathbf{K}_\times$

E Elastic contribution by means of Sparse Inverse Distance Weighting (SIDW)

$$\Delta \mathbf{x}_k = \sum_{j=0}^{N_b} \frac{\text{IDW}_{(k,j)}}{|\text{IDW}_{(k,:)}|} \boldsymbol{\varepsilon}_j \quad \forall k = [1, N_v] \quad \text{with} \quad \text{IDW}_{(k,j)} = \frac{1}{\|\mathbf{x}_k - \mathbf{x}_j\|^p}$$

memory/efficiency trade-off sparse fix: $\text{SIDW}_{(k,j)} = \text{IDW}_{(k,j)}$ if $\text{IDW}_{(k,j)} > \xi$

T Residuals (if any) simulated by means of Transpiration boundary conditions